THE JOURNAL OF BIOLOGICAL CHEMISTRY VOL. 285, NO. 9, pp. 6538–6551, February 26, 2010

G Protein $\beta\gamma$ Subunits Regulate Cell Adhesion through Rap1a and Its Effector Radil[S]

Received for publication, September 24, 2009, and in revised form, December 21, 2009 Published, JBC Papers in Press, January 4, 2010, DOI 10.1074/jbc.M109.069948

Syed M. Ahmed[‡1], **Avais M. Daulat**[‡], **Alexandre Meunier**[‡], **and Stephane Angers**[‡§2]

From the [‡]*Department of Pharmaceutical Sciences, Leslie Dan Faculty of Pharmacy, and the* [§]*Department of Biochemistry, Faculty of Medicine, University of Toronto, Toronto, Ontario M5S 3M2, Canada*

The activation of several G protein-coupled receptors is known to regulate the adhesive properties of cells in different contexts. Here, we reveal that G$\beta\gamma$ subunits of heterotrimeric G proteins regulate cell-matrix adhesiveness by activating Rap1a-dependent inside-out signals and integrin activation. We show that G$\beta\gamma$ subunits enter in a protein complex with activated Rap1a and its effector Radil and establish that this complex is required downstream of receptor stimulation for the activation of integrins and the positive modulation of cell-matrix adhesiveness. Moreover, we demonstrate that G$\beta\gamma$ and activated Rap1a promote the translocation of Radil to the plasma membrane at sites of cell-matrix contacts. These results add to the molecular understanding of how G protein-coupled receptors impinge on cell adhesion and suggest that the G$\beta\gamma$·Rap1·Radil complex plays important roles in this process.

G protein-coupled receptors (GPCRs)[3] form the largest family of cell surface signal transducing molecules in vertebrates. The regulation of cell migration as well as cell-cell and cell-matrix adhesion by GPCRs is essential for normal embryonic development (1–3) and is important for several cellular processes in adults such as immune response (4–6), hemostasis (7, 8), and vascular integrity (3, 9). The activation of chemokine receptors, for example, has been well demonstrated to regulate directional cell migration and cell-matrix adhesion in the context of various immune functions (10) but also during several other instances of cell motility (11, 12). The activation of platelets at sites of vascular wall injury is another context where GPCR signaling is involved in regulating cell adhesion with the extracellular matrix (13). Revealing the importance of these processes, defects in GPCR signaling downstream of pro-migratory or adhesive signals have been linked with different human diseases including inflammation (14–17) and cancer metastasis (18–20).

Because pertussis toxin-sensitive Gα_i-activated pathways are thought to play important roles downstream of GPCRs during migration and adhesion, the G$\beta\gamma$ subunits of the heterotrimeric G proteins can be predicted to play integral signaling functions during these processes. Supporting this, G$\beta\gamma$ subunits are known to associate and potentiate the activity of the p110β and -γ isotypes of phosphoinositide 3-kinase that regulate directed cell migration (21, 22) by facilitating the polarized recruitment of downstream signaling proteins, which leads to cytoskeleton remodeling. The discovery that PLIC-1 interferes with chemokine receptor-mediated chemotaxis by sequestering G$\beta\gamma$ and hindering its normal cellular functions as well as evidence implicating G$\beta\gamma$ in cell invasion and spreading further highlights the importance of G$\beta\gamma$ in cell movement (23, 24). However, the precise molecular mechanisms by which GPCRs and G$\beta\gamma$ impinge on cell motility remain incompletely understood especially with respect to the dynamic control of cell adhesiveness.

In all instances of cell motility, cells constantly need to alter their interactive associations with the extracellular matrix in response to environmental cues. Central to this process is the regulation of integrin avidity and affinity for matrix protein components (11, 25, 26). The small GTP binding protein Rap1 is implicated in the "inside-out" signaling that rapidly leads to integrin activation. For example, overexpression of the constitutively active mutant Rap1aQ63E leads to increased cell adhesion (27) and integrin activation (28) by inducing a change in the conformation of the extracellular region of integrins. This unclasping of the inhibitory interaction between the α and β integrins switches their affinity for the extracellular matrix to a high affinity state. Although Rap1-induced inside-out signaling has been deemed important in the context of GPCR signaling during platelet and leukocyte activation (13, 29–33), how this signaling and integrin activation are regulated by GPCRs and whether it extends to other cellular contexts is not well understood.

Despite significant indirect evidence positioning G$\beta\gamma$ subunits as functional regulators of cell motility and adhesion downstream of GPCR activation, our understanding of the molecular mechanisms underlying their roles in these processes is incomplete. In the present study we, thus, employed a functional proteomic approach to further interrogate how

[S] The on-line version of this article (available at http://www.jbc.org) contains supplemental Fig. 1 and a table.

[1] Supported by an Alexander Graham Bell Canada Graduate Scholarship from the Natural Sciences and Engineering Research Council and recipient of an Ontario Graduate Scholarship in Science and Technology.

[2] Canada Research Chair in Functional Architecture of Signal Transduction. Supported by the Canadian Institutes of Health Research and the Cancer Research Society. To whom correspondence should be addressed: Leslie Dan Faculty of Pharmacy, University of Toronto, 144 College St., Toronto, Ontario M5S 3M2, Canada. Tel.: 416-978-4939; Fax: 416-978-8511; E-mail: stephane.angers@utoronto.ca.

[3] The abbreviations used are: GPCR, G protein coupled receptor; DIL, diluted domain; FPR, formyl peptide receptor; PDZ, domains found in PSD-95, Dlg ZO-1; RA, Ras association domain; RalGDS-RBD, RalGDS-Ras binding domain; RAP1GAP, Rap1 GTPase-activating protein; Strep, streptavidin; PTX, pertussis toxin; fMLP, formyl-Met-Leu-Phe peptide; PBS, phosphate-buffered saline; ANOVA, analysis of variance; GFP, green fluorescent protein; DMEM, Dulbecco's modified Eagle's medium; siRNA, small interfering RNA; GST, glutathione *S*-transferase; HA, hemagglutinin; TAP, tandem affinity purification.

Gβγ subunits mediate their actions. We identify Rap1a and its effector Radil as novel Gβγ-associated proteins and present evidence functionally implicating this protein complex downstream of GPCR activation for the control of cell-matrix adhesion.

EXPERIMENTAL PROCEDURES

Plasmid Constructs and Reagents—Human $G\beta_2$, Radil, and Rap1GAP cDNAs were cloned from a human brain cDNA library in the pGlue or pIRES-puro-FLAG backbone vector (34). All PCR-amplified regions were verified by DNA sequencing. pCGN HA-Rap1aQ63E was obtained from J. Cooper (University of Washington, Seattle, WA), and pMT2 Rap1aG12V and pCDNA3.1 FLAG-HA-AF6 were provided by J. L. Bos (University Medical Center Utrecht, The Netherlands). A detailed description of the different plasmids, maps, and sequences will be provided upon request. Formyl-Met-Leu-Phe peptide (fMLP) was purchased from Biomol. Pertussis toxin was purchased from Tocris Bioscience. Antibodies were purchased from the following vendors: α-HA.11 (Covance), α-FLAG (Sigma), α-Gβ (T20) (Santa Cruz Biotechnology), α-Rap1a (C-17) (Santa Cruz Biotechnology), α-Erk1/2 (Cell Signaling), α-CD29 monoclonal antibody (9EG7) (BD Transduction Laboratories), α-GFP (Covance and the University of Alberta), α-tubulin (Sigma), and α-Na-K-ATPase (Affinity Bioreagents).

Tissue Culture and Transfection—HEK293T and HT1080 cells were grown in Dulbecco's modified Eagle's medium (DMEM; Sigma) supplemented with 10% fetal bovine serum (Sigma) and penicillin/streptomycin (Sigma) in a 37 °C humidified incubator with 5% CO_2. Stable cell lines were generated by calcium phosphate transfection followed by puromycin selection (2 μg/ml). cDNA transfections in HT1080 cells were done using Lipofectamine 2000 (Invitrogen) at a 1:2 ratio (cDNA:Lipofectamine 2000) or polyethyleneimine at a 1:3 ratio at 70% cells confluency with a typical 80–90% transfection efficiency. siRNAs were delivered at a final concentration of 50 nM in HT1080 cells by reverse transfection using Lipofectamine RNAiMax (Invitrogen) according to the manufacturer's protocol. The siGenome Non-Targeting siRNA (control siRNA) and human Radil ON-TARGET plus SMARTpool siRNA (hRadil siRNA pool) were purchased from Thermo Scientific, and the single siRNA targeting human Radil (hRadil siRNA #1) was purchased from Ambion Inc. The sequences for each siRNA in the ON-TARGET plus SMARTpool (Thermo Scientific) for human Radil are GCACAGGAACCCACUACAA, GAGCGUACUCUUCCCUUGA, CGUCAUGGCGGGAAGAAGA, and GAAGGUUUAUCCCGGAGGU. The sequence for human Radil siRNA #1 (Ambion) is GGUUUAUCCCGGAGGUUUG. The sequence for siGENOME Non-Targeting siRNA #4 (Thermo Scientific) is AUGAACGUGAAUUGCUCAAUU.

Production of Radil Antibody—A rabbit polyclonal antibody was raised against full-length recombinant human Radil protein. Human Radil coding sequence was cloned into pGEX vector (Promega) downstream of GST. Proteins were expressed in BL-21 *Escherichia coli* strain upon stimulation with isopropyl 1-thio-β-D-galactopyranoside (500 μM; Sigma) in a shaker at room temperature (240 rpm) overnight. The bacterial pellet was lysed by sonication in buffer containing 20 mM Tris-HCl, pH 8.0, 200 mM NaCl, 5 mM dithiothreitol, 1 mM phenylmethylsulfonyl fluoride, and proteins purified on Glutathione-Sepharose 4B (GE Healthcare). The purity of the purified Radil protein was confirmed by SDS-PAGE and mass spectrometry analysis and provided to Covance Custom Immunology Services for antibody production. The final antisera was purified first by negative selection by running the crude antisera through GST proteins immobilized on a glutathione-Sepharose 4B column followed by affinity purification on a GST-Radil-glutathione-Sepharose 4B column. The antibody was characterized for antigen specificity by enzyme-linked immunosorbent assay (Covance Custom Immunology Services) and by Western blotting lysates from Radil siRNA-treated cells.

Tandem Affinity Purification and Mass Spectrometry—HEK293T cells (2×10^8) expressing tandem affinity purification (TAP)-tagged $G\beta_2$, $G\gamma_2$, or Radil constructs were used for the TAP procedure as described previously (34). Briefly, cells were lysed and solubilized in TAP lysis buffer (0.1% Igepal CA630, 10% glycerol, 50 mM Hepes-NaOH, pH 8.0, 150 mM NaCl, 2 mM EDTA, 2 mM dithiothreitol, 10 mM NaF, 0.25 mM $NaOVO_3$, 50 mM β-glycerophosphate, and protease inhibitor mixture (Calbiochem)), and extracts were incubated at 4 °C with 100 μl of packed streptavidin (GE Healthcare) or α-FLAG M2 (Sigma) resin. The resin was washed, and protein complexes were then eluted from the streptavidin resin in calmodulin binding buffer (50 mM Hepes-NaOH, pH 8.0, 150 mM NaCl, 10 mM β-mercaptoethanol, 1 mM magnesium acetate, 1 mM imidazole, 0.1% Nonidet P-40) supplemented with 2 mM biotin (Sigma). The second round of affinity purification was performed using 100 μl of calmodulin resin (GE Healthcare) followed by elution in calmodulin elution buffer (25 mM EGTA, 50 mM ammonium bicarbonate). α-FLAG immunoprecipitation for mass spectrometry analysis-purified proteins were eluted from the beads using 500 mM ammonium hydroxide at pH 11.0. The proteins in the complex were reduced in 25 mM dithiothreitol and alkylated using 100 mM iodoacetamide (Sigma) and brought to 1 mM $CaCl_2$. The proteins were then directly digested with sequencing-grade trypsin (Promega). The resulting peptide mixture was then analyzed by liquid chromatography- tandem mass spectrometry using a LTQ-XL Linear Ion Trap Mass spectrometer (Thermo Scientific). The acquired tandem mass spectra were searched against a FASTA file containing the human NCBI sequences using a normalized implementation of SEQUEST running on the Sorcerer platform (Sage-N Research). The resulting peptide identifications returned by SEQUEST were filtered and assembled into protein identifications using peptide and protein prophets (Institute of Systems Biology, Seattle).

Affinity Purification, Immunoprecipitation, and Western Blot—Cells were lysed (0.5% Igepal CA630, 20 mM Tris-HCl, pH 7.5, 150 mM NaCl, 2 mM EDTA, and protease inhibitor) and incubated at 4 °C for 20 min to solubilize the proteins. Affinity purification and immunoprecipitations were performed using streptavidin resin (GE Healthcare) or FLAG-M2 beads (Sigma) for 1 h at 4 °C. After extensive washes with lysis buffer, the beads were eluted with 2× Laemmli sample buffer and heated at 95 °C for 5 min in the presence of β-mercaptoethanol

(Sigma). Whole cell lysates or purified protein samples were resolved by SDS-PAGE and transferred onto nitrocellulose transfer membranes (Pall Corp.). Western blotting was performed with antibodies as indicated in the figure legends (Figs. 1–3, 6, and 7) followed by chemiluminescent detection with SuperSignal West Pico (Thermo Scientific) and exposed on film.

Immunocytochemistry and Confocal Microscopy—HEK293T and HT1080 stably expressing Venus-Radil were transfected with HA-Rap1a, HA-Rap1aG12V, HA-Rap1aQ63E, or FLAG-$G\beta_2$ and $G\gamma_2$ as indicated. For intracellular protein staining, cells were fixed in 4% paraformaldehyde and permeabilized with 0.2% Triton X-100 in phosphate-buffered saline (PBS) supplemented with 10% normal donkey serum. Samples were then immunostained with α-HA (HA.11, Covance) or α-FLAG (Sigma)-specific mouse monoclonal antibodies in PBS supplemented with 1% normal donkey serum. Cells were subsequently labeled with secondary goat-anti-mouse antibody conjugated to Alexa Fluor 594 (Invitrogen) to visualize HA-tagged Rap1a or FLAG-tagged $G\beta_2$. The coverslips were mounted onto slides using Vectashield mounting media (Vector Laboratories). Cells were visualized, and images were acquired with a Carl Zeiss LSM510 confocal microscope using a Plan-Apochromat 63×/1.4 oil immersion objective. Lasers at a 488- and 543-nm wavelength were fired independently using the multi-track function of LSM510. Uncompressed images were processed using Zeiss LSM Image browser Version 4.2. To magnify portions of the plasma membrane to depict co-localization, images were cropped as designated in Fig. 3*A* (in *white boxes*) using Adobe Photoshop CS3. For fMLP stimulation experiments, HT1080 cells stably expressing Venus-Radil were serum-starved for 24 h and stimulated with fMLP (1 μM) for the indicated times at 37 °C. After treatments, cells were immediately chilled on ice and washed once with ice-cold PBS followed by fixation in 4% paraformaldehyde for 30 min at room temperature.

Subcellular Fractionation—HT1080 cells transiently transfected with the indicated cDNAs in 100-mm tissue culture dishes were washed with PBS, pH 7.4, and lysed by Dounce homogenization (20 strokes) in hypotonic buffer (5 mM Tris-HCl, 2 mM EDTA). A small fraction was separated into aliquots from each sample and labeled as "inputs." The lysates were centrifuged at 1000 × *g* for 5 min at 4 °C to remove unbroken cells and nuclei. The post-nuclear supernatant was transferred to a new tube followed by centrifugation at 100,000 × *g* (34,100 RPM in Ti90 rotor) for 30 min. The supernatant was removed, and the pellet was resuspended in the above buffer and subjected to a second round of centrifugation at 100,000 × *g* for 30 min. The supernatant was discarded, and the pellet containing the membrane fraction was resuspended in the above lysis buffer. Equal amounts of proteins for each the input and membrane fractions were then resolved by SDS-PAGE for Western blot analysis. An antibody against Na-K-ATPase was used as internal loading control.

Cell Spreading Assay—HT1080 cells were plated on glass coverslips and transfected with GFP alone, Venus-Rap1GAP, or GFP together with different expression plasmids coding for HA-Rap1aQ63E, HA-Radil, or HA-Gβ and untagged Gγ. 48 h after transfections, cells were fixed in 4% paraformaldehyde and immunostained with α-HA monoclonal antibody to label the overexpressed proteins followed by secondary detection with goat-anti-mouse conjugated Alexa 594. Cells were mounted on slides and visualized under a 63× oil immersion lens using a Carl Zeiss LSM 510 confocal microscope. Spreading of cells co-expressing GFP and the overexpressed protein of interest was quantified by measuring the area of each cells using Image J software. To acquire more quantitative and real-time insights into cell adhesion and spreading, we employed a change in impedance as a measure of the degree of cell attachment and spreading using the xCELLigence system (Roche Applied Science). HT1080 cells were transfected with the different plasmids. 48 h after transfections, cells were trypsinized and resuspended in DMEM containing 10% fetal bovine serum. 25,000 cells from each condition were seeded onto a 96-well microtiter xCELLigence assay plate (E-Plate) (ACEA Biosciences Inc.) and placed on the Real-time xCELLigence Cell Analyzer (Roche Applied Science) platform at 37 °C to measure the "cell index" every 5 min. The cell index unit is defined as $(R_n - R_b)/15$, where R_n is the cell electrode impedance of the well when it contains cells, and R_b is the background impedance of the well with the media alone.

Cell Adhesion Assay—96-well flat-bottom plates (BD Biosciences) were coated with 5 μg/ml fibronectin from bovine plasma (Sigma) for 16 h at 4 °C. Wells were washed and blocked with a solution of 2% filtered bovine serum albumin in PBS for 1 h at room temperature. 48 h after transfection with cDNA or siRNAs, HT1080 cells were dissociated from culture plates with trypsin, washed twice with PBS, and resuspended in serum free DMEM supplemented with 0.1% bovine serum albumin and 20 mM HEPES, pH 7.4. Before the adhesion assay the cells were incubated at room temperature for 1 h on a nutating shaker. Where indicated, cells were incubated at 37 °C for 1 h with the indicated drugs. For pertussis toxin (PTX) treatment, cells were incubated overnight in 10% fetal bovine serum, DMEM media containing 100 ng/ml PTX. Cells were plated in triplicate at a density of 2.5×10^4 per well and allowed to adhere for 8 min at 37 °C followed by washing with warm 0.2% bovine serum albumin in PBS. For each condition, input controls were let to adhere for 30 min followed by aspiration of the media and fixation. Cells were fixed with glutaraldehyde (Sigma) for 20 min and stained with hematoxylin Gill's No.1 reagent (Sigma) followed by washing with acid alcohol (0.5% hydrochloric acid in 70% ethanol) to remove residual the stain and 0.04% ammonium hydroxide for color maturation. Cell adhesion was quantified by taking a minimum of three random pictures per well. Cells in each picture were then counted using an automated macro algorithm created in ImageJ Version 1.41 software.

Integrin Activation Assay—HT1080 cells were resuspended as described for adhesion assay and let to recover at 37 °C for 45 min. Transfected or drug-treated cells were incubated for 1 h in the presence of α-CD29 (9EG7) antibody (BD Biosciences). Cells were washed in PBS three times and incubated in the presence of Dylight™-488-conjugated donkey α-rat IgG (Jackson ImmunoResearch Laboratories) for 45 min followed by three washes in PBS. Cells were then fixed in 4% paraformaldehyde for 15 min and resuspended in PBS. Flow cytometry analysis was performed on a Beckman

Coulter Cytomics FC500 MPL analyzer using the CXP 2.2 software. Post acquisition data analysis was done with FlowJo Version 7.2.5 software (Tree Star Inc).

Rap Activation Assay—HT1080 cells were serum-starved for 16 h followed by stimulation with 100 nM fMLP for different time points as indicated. After three washes with PBS, the cells were lysed in TAP lysis buffer containing protease and phosphatase inhibitors (10 mM NaF, 0.25 mM $NaOVO_3$, 50 mM β-glycerophosphate). 800 μg of proteins was then incubated with GST-RalGDS-RBD coupled to glutathione-Sepharose 4B beads for 1 h at 4 °C. Beads were then washed 3 times in TAP lysis buffer, bound proteins were eluted in 15 μl of 2× Laemmli buffer containing β-mercaptoethanol (Sigma), and samples were analyzed by Western blot analysis using α-Rap1a antibodies. A fraction of whole cell lysate was also analyzed by Western blot to assess total Rap1a.

Statistical Analysis—Data reported as ±S.E. were analyzed by analysis of variance (ANOVA) followed by Tukey's post hoc multiple comparison tests (Graphpad Prism 5 software). Statistical significance was measured at $p < 0.05$ for all analysis.

RESULTS

Proteomic Identification of Radil and Rap1a as Novel Effectors of Gβγ Subunits of Heterotrimeric G Proteins—To identify novel effectors of Gβγ subunits of heterotrimeric G proteins, $Gβ_2$ and $Gγ_2$ cDNAs were cloned downstream of streptavidin (Strep)- and calmodulin-binding peptides in the pGLUE vector (35), and stable human embryonic kidney (HEK293T) cells expressing low levels of Gβ or Gγ fusion proteins were derived. Extracts from these cells were subjected to tandem affinity chromatography to isolate $Gβ_2$ and $Gγ_2$ protein complexes. These protein complexes were digested in solution with trypsin, and the resulting peptide mixture was analyzed by liquid chromatography-tandem mass spectrometry. The detailed list of proteins identified in the complexes is listed in the supplemental table and is schematically represented in Fig. 1*A*. Many peptides corresponding to several Gα subunits were predictably found in both Gβ- and Gγ-purified complexes. Furthermore, most Gγ subunits and Gβ subunits were found to associate with $Gβ_2$ and $Gγ_2$, respectively. Based on the total number of peptides identified and derived sequence coverage, the data also support previous reports that DnaJ (36, 37), the t-complex polypeptide (TCP) complex (38), and phosducin-like proteins (39) associate with either fully formed or nascent Gβγ subunits.

In terms of the total peptides identified, the recently identified Rap effector Radil (40) was one of the most abundant proteins found in both $Gβ_2$ and $Gγ_2$ protein complexes. Of note, a few peptides attributed to Rap1a were also present in the $Gβ_2$ pulldown experiment (Fig. 1*A* and the supplemental table). The reciprocal analysis of Radil protein complexes by mass spectrometry agreed with the previous showing that Radil interacts with the Rap family of small GTPases (40) and confirmed the association of Radil with Gβγ heterodimers as several peptides corresponding to the different Rap isoforms as well as Gβ and Gγ subunits were identified (Fig. 1*A* and the supplemental table). The Radil affinity purification/mass spectrometry experiments were performed in HEK293T and HT1080 fibrosarcoma cells with similar results (supplemental table).

Co-affinity purification and Western blot experiments were then performed to support and validate the mass spectrometry data. Lysates from control HEK293T cells or from cells stably expressing Strep-HA-$Gγ_2$ or Strep-HA-Radil were subjected to affinity purification using Sepharose-streptavidin followed by Western blotting using antibodies specific to Radil, HA, Gβ, or Rap1. Confirming the mass spectrometry results, endogenous Gβ and Rap1 were detected in purified Radil complexes (Fig. 1*B*, *left panel*), and endogenous Radil and Gβ proteins were detected in $Gγ_2$ samples (Fig. 1*B*, *right panel*).

Radil is a protein of 1075 amino acids composed of a RA (Ras-associating) domain known to bind small GTP-binding proteins of the Ras family, a central DIL (Diluted) domain of unknown function, and a PDZ domain at the C terminus (Fig. 1*C*). To test for specificity of the association between Radil and Gβγ, the interaction between AF6 and Gβγ was addressed (Fig. 1*C*). AF6 is a protein related to Radil sharing its domain architecture and has been similarly reported to interact with Rap1a and play important roles in cell adhesion (41–43). Whereas endogenous Gβ could be co-immunoprecipitated with Radil, it was absent from AF6 or control immunoprecipitates (Fig. 1*C*, compare *lane 6* with *lanes 4* and *5*). We conclude that the Rap effector Radil is a novel Gβγ-associated protein.

Radil Recruits Gβγ and Activated Rap1a in the Same Protein Complex—Because only a few peptides for Rap1a were identified in the Gβ and Gγ pulldown assays and several hundred in Radil complexes, the interaction between Gβ and Rap1 is likely indirect and mediated by Radil. To examine this possibility, $Gβ_2$ was purified from cells exogenously expressing Rap1 alone or from cells overexpressing both Rap1 and Radil. Whereas trace amounts of Rap1 were co-purified with $Gβ_2$ in cells expressing these proteins, the overexpression of Radil strongly promoted the association of Rap1 with $Gβ_2$ (Fig. 2*A*, compare *lanes 2* and *3*). Radil was previously shown to selectively interact with the activated GTP-bound form of Rap1 and exhibit negligible affinity for its inactive GDP-bound form (40). To determine whether the activation state of Rap1 is important for the binding of Gβ to Radil, we first established that overexpression of Rap1GAP, a GTPase-activating protein (GAP) specific for Rap1 (44, 45), could block the association of Radil with Rap1a (Fig. 2*B*, compare *lanes 2* and *3*). Similarly, whereas Gβ is efficiently co-purified with Radil in control cells, this association is markedly attenuated in Rap1GAP-overexpressing cells (Fig. 2*B*). We also performed the reciprocal experiment and showed that expression of the constitutively activated Rap1aQ63E promoted the association of Gβγ with Radil (Fig. 2*C*). We conclude that after Rap1 activation, Radil interacts with Rap1 and can recruit Gβγ into the complex.

Gβγ and Rap1 Promote the Recruitment of Radil at Sites of Cell-Matrix Adhesion—The activation of several GPCRs has previously been shown to activate Rap1a in multiple contexts (29, 46–51). Our results describing Gβγ forming a protein complex with Rap1a, and its effector Radil is consistent with Gβγ participating in Rap1a-dependent processes. Upon activation, Rap1 translocates from a cytoplasmic pool to the plasma membrane (52, 53). Rap effectors are subsequently recruited to this activated membrane pool of Rap1 to in turn exert their biological functions (54, 55). To test if the subcellular localization of Radil changes upon Rap1 activation and Gβγ overex-

pression, we performed subcellular localization microscopy experiments in HT1080 fibrosarcoma cells stably expressing a Venus-Radil fusion protein. We chose this model system because Radil expression is known to be induced after an oncogenic translocation in a pediatric sarcoma (40), and its functions may be particularly relevant in this cellular context. In the resting state, Radil appears to be mainly localized in a cytoplasmic pool with minimal plasma membrane localization (Fig. 3*A*, *panel c*). In contrast, overexpression of wild-type Rap1a (Fig. 3*A*, *panels e–g*) or two different constitutively active Rap1a

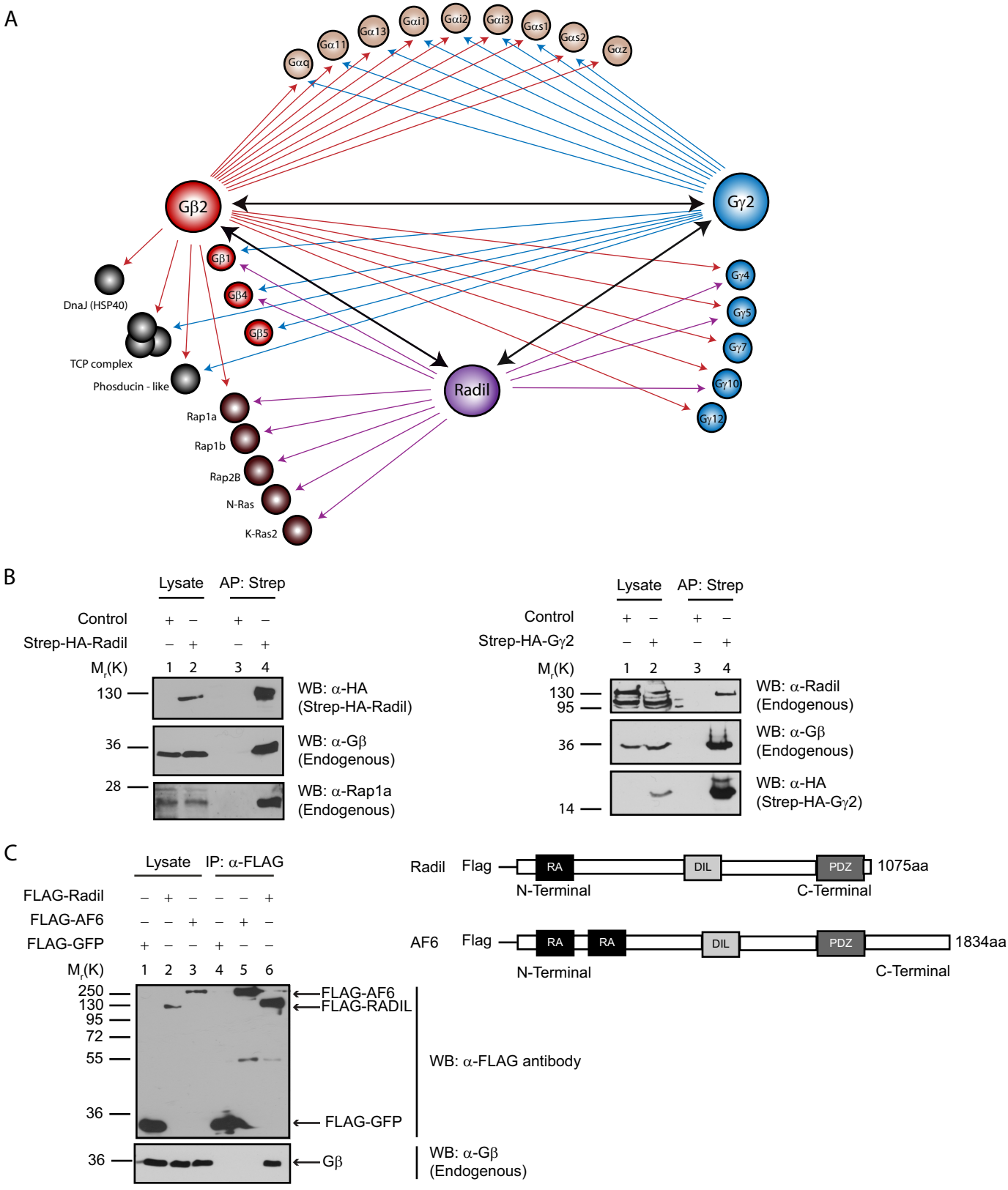

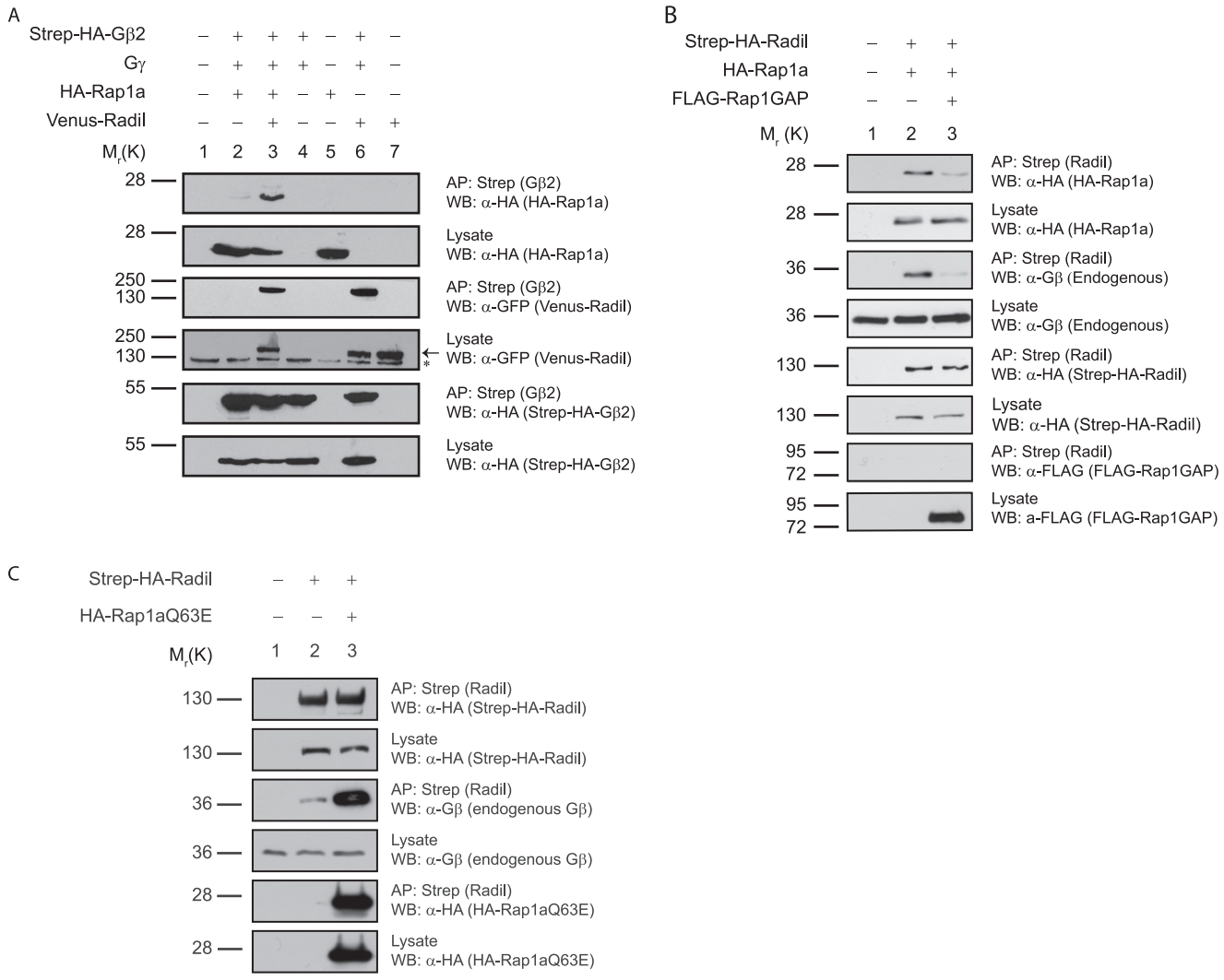

FIGURE 2. **Interaction between Gβγ, Rap1a, and Radil.** *A*, Radil physically connects Gβγ and Rap1a. HEK293T cells were transfected with different plasmid combinations coding for Strep-HA-$G\beta_2$, $G\gamma_2$, HA-Rap1a, and Venus-Radil. Strep-HA-$G\beta_2$-containing complexes were affinity-purified with streptavidin-Sepharose beads, and the association with Rap1a and Radil was monitored by Western blot (*WB*) with α-HA and α-GFP antibodies, respectively. The efficiency of $G\beta_2$ purification and expression was also followed by Western blot using HA antibodies. A fraction of the lysates for each samples was probed with α-HA or α-GFP antibodies to assess protein expression. The association of Rap1a with $G\beta_2$ was enhanced when Radil was overexpressed (compare *lanes 2* and 3) ($n = 3$). *, nonspecific band. *B*, formation of the Gβγ·Rap1a·Radil complex requires active Rap1a. HEK293T cells were transfected with expression plasmids for Strep-HA-Radil and HA-Rap1a only (*lane 2*) or together with a vector coding for FLAG-Rap1GAP (*lane 3*). Strep-HA-Radil was purified using streptavidin-Sepharose beads, and its association with Rap1 and Gβ was monitored by a Western blot using α-HA and α-Gβ antibodies, respectively. The expression of Rap1GAP was followed using α-FLAG antibodies. Although HA-Rap1a and Gβ bound to Strep-HA-Radil (*lane 2*), these interactions were compromised in the presence of overexpressed FLAG-Rap1GAP (*lane 3*) ($n = 4$). *C*, expression of a constitutively active Rap1a mutant (Rap1aQ63E) promotes the interaction of Gβ with Radil. Strep-HA-Radil expressing stable cells were transfected or not with HA-Rap1aQ63E. 48 h after transfection, Radil was affinity-purified with streptavidin-Sepharose beads for 1.5 h, and the eluates were analyzed by Western blot using the indicated antibodies. Untransfected HEK293T cells were used as the negative control for streptavidin purification. *AP*, affinity purification. M_r, molecular weights. *K*, ×1000.

mutants (Fig. 3*A panels*, *h–m*) led to the translocation of Radil to the plasma membrane with extensive co-localization with the activated pool of Rap1a. Note that although expressing wild-type Rap1a was sufficient to translocate Radil, this effect was significantly stronger with the constitutively active Rap1a mutants (data not shown). These results support previous data

FIGURE 1. **Identification of Radil as a novel interactor of Gβγ subunits of heterotrimeric G proteins.** *A*, shown is the protein-protein interaction network of $G\beta_2$, $G\gamma_2$, and Radil. *Single-headed arrows* represent interactions found in $G\beta_2$ (*red*), $G\gamma_2$ (*blue*), and Radil (purple) pulldown experiments, color coded according to the color of the bait. *Dark double-sided arrows* represent proteins reciprocally identified using the other as bait. $G\beta_2$ ($n = 3$), $G\gamma_2$ ($n = 2$), and Radil pulldown assays ($n = 2$) were performed in HEK293T and HT1080 cells. Analysis of the tandem affinity-purified $G\beta_2$ or $G\gamma_2$ protein complexes using mass spectrometry reveals several known Gβγ interactors. The small GTP-binding protein Rap1a and the newly characterized protein Radil were also identified in the $G\beta_2$ complexes. The reciprocal analysis of Radil protein complexes confirmed Radil as a Gβγ-associated protein and also revealed that it binds small G proteins of the Ras family. *B*, streptavidin affinity purification (*AP*) of Strep-HA-Radil (*left panel*) and Strep-HA-$G\gamma_2$ (*right panel*) and immunodetection of co-purified endogenous Gβ, Rap1a, or Radil as indicated validates the mass spectrometry results. *WB*, Western blot. *C*, *left panel*, HEK293T cells were transiently transfected with expression vectors coding for FLAG-GFP, FLAG-Radil, or the closely related FLAG-AF6, and proteins were immunoprecipitated (*IP*)using α-FLAG M2-conjugated agarose beads followed by a Western blot with α-FLAG (*top panel*) or α-Gβ (*bottom panel*) antibodies ($n = 3$). Gβ co-immunoprecipitates with FLAG-Radil but not with FLAG-GFP or FLAG-AF6. *Right panel*, a schematic representation of Radil and AF6 proteins shows the similarity between the two proteins containing RA, DIL, and PDZ domains.

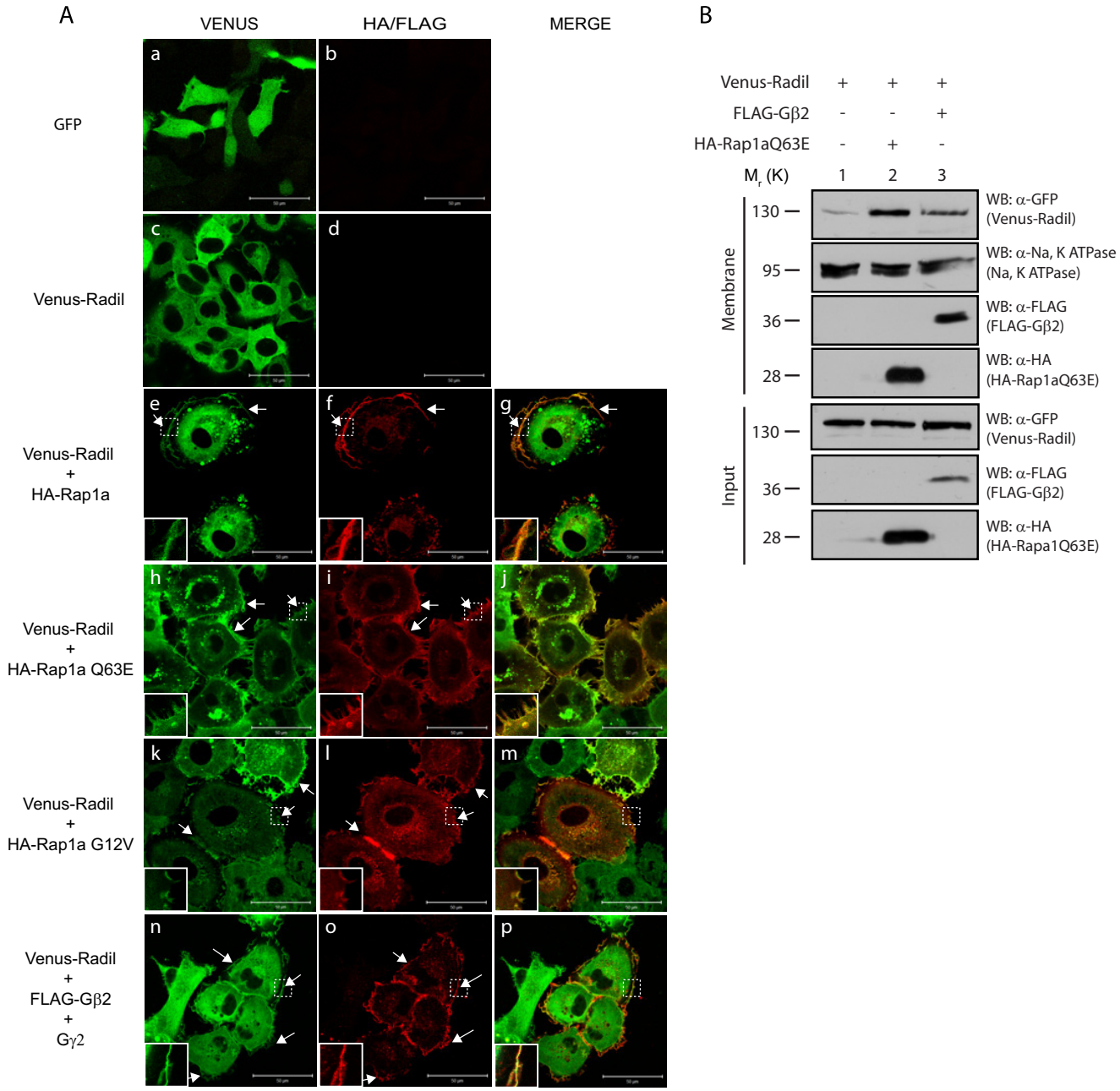

FIGURE 3. **Rap1a-GTP and Gβγ promote the translocation of Radil at cell-matrix contacts in HT1080 cells.** *A*, shown is localization of GFP (*a* and *b*), Venus-Radil (*c* and *d*), or Venus-Radil co-expressed with wild-type HA-Rap1 (*e–g*), HA-Rap1aQ63E (*h–j*), HA-Rap1G12V (*k–m*), or FLAG-Gβ_2/Gγ1 (*n–p*). HA- and FLAG-tagged Rap1a or Gβ_2 + Gγ (untagged) were transiently transfected in HT1080 cells stably expressing Venus-Radil as indicated. Cells were fixed followed by immunodetection with α-HA (*e–m*) or α-FLAG (*n–p*) monoclonal antibody followed by secondary detection with goat-anti-mouse conjugated to Alexa 594 antibody. Cells were visualized using a Zeiss LSM 510 confocal microscope under 63× oil immersion objective. *White arrows* depict plasma-membrane co-localization. *White boxes* indicate magnified sections cropped in Adobe Photoshop CS3. Images shown are representative of 10–15 cells analyzed in three independent experiments. *Bars*, 50 μm. *B*, membrane fractions show enrichment of Venus-Radil when Rap1aQ63E and Gβγ are expressed. HT1080 cells stably expressing Venus-Radil were transiently transfected to express the indicated proteins. Cells were lysed in hypotonic buffer and subjected to subcellular fractionation as described under "Experimental Procedures." Membrane fractions and the inputs were analyzed by Western blot (*WB*) to determine the amount of Venus-Radil present in the membrane pool when HA-Rap1aQ63E or FLAG-Gβ_2 was co-expressed. The blot for the membrane fractions was stripped and re-probed using α-Na-K-ATPase antibody to provide for an internal loading control.

that Radil forms a complex with the GTP-bound form of Rap1a (Fig. 2*B*) (40). Interestingly, at the plasma membrane, Radil appears to be enriched in both lamellipodia and filopodia (Fig. 3*A*, *insets*) a subcellular localization compatible with a role in cell-matrix interactions and cell migration. We next asked if overexpression of Gβγ impacts on the localization of Radil. Gβγ is predominantly localized to the plasma membrane in these cells (Fig. 3*A*, *panel o*), and overexpression of Gβ_2 and Gγ_2 phenocopied Rap1a expression in that it resulted in translocation of Radil to the plasma membrane (Fig. 3*A*, *panels n–p*). As control, we showed that overexpression of activated Rap1aQ63E did not lead to the membrane enrichment of wild-type GFP, which localizes to the cytosol and nucleus of these cells (supplemental Fig. 1). Also, we demonstrated that overex-

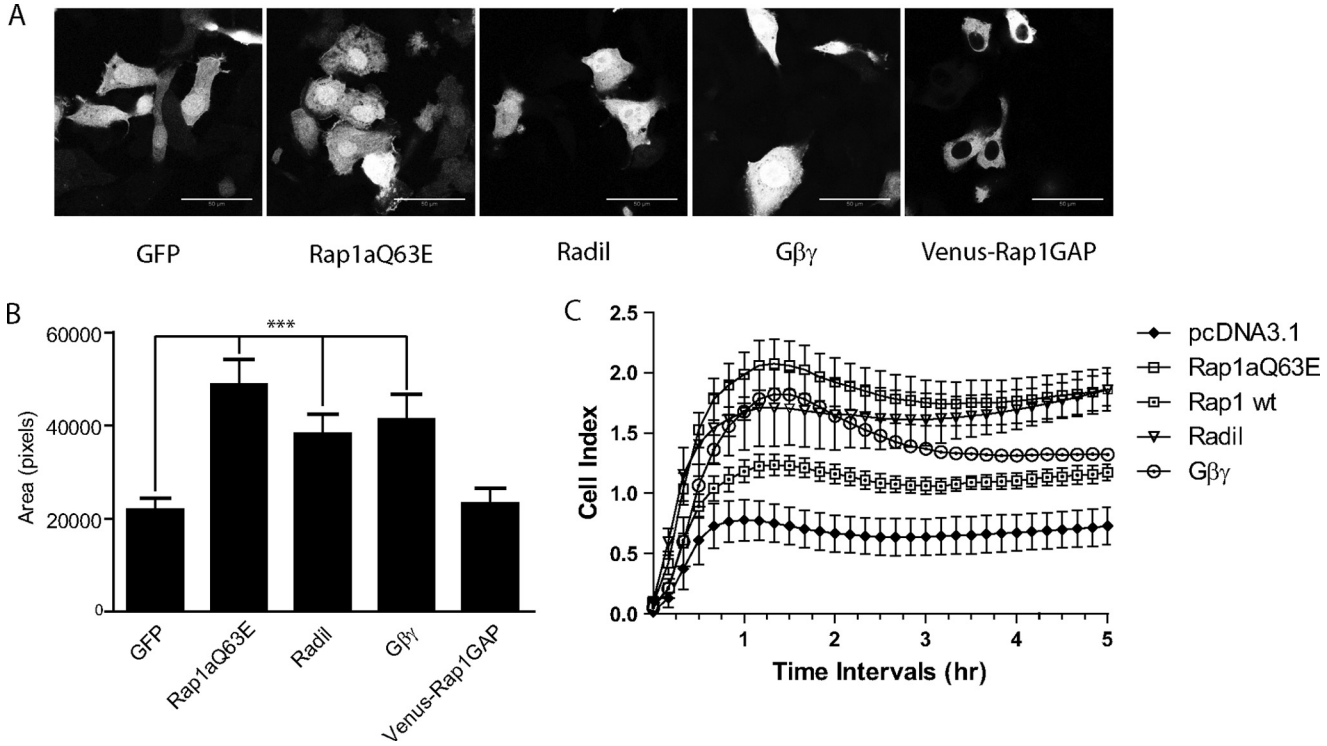

FIGURE 4. **The Gβγ·Rap1·Radil complex increases HT1080 cell spreading.** *A*, HT1080 cells were plated on coverslips and transiently transfected with cDNA for GFP alone or together with HA-Rap1aQ63E, HA-Radil, and HA-$G\beta_2$+Gγ. Cells transfected with Venus-Rap1GAP alone were also used as a control. 48 h post-transfection cells were fixed and visualized using a confocal microscope under 63× oil immersion objective. *Bars*, 50 μm. *B*, the spreading of cells co-expressing GFP and the indicated proteins was quantified by taking the total surface area for each cells using the Image J software. A total of 50–70 cells were analyzed. *Error bars* represent ± S.E. Statistical significance was analyzed using one-way ANOVA followed by Tukey's multiple comparison test; $p < 0.05$. *C*, HT1080 cells were transfected with the indicated cDNAs. 48 h post-transfections cells were trypsinized and resuspended in DMEM, 10% fetal bovine serum media. Cells were counted, 25,000 cells were plated on a 96-well xCELLigence microtiter plate (E-Plate), and the change in cell index was measured using the xCELLigence impedance system. *Error bars* represent ±S.D. Data shown are representative of two independent experiments. *wt*, wild type.

pression of an active form of Rac1, which is a Rho family GTPase with described roles in cell migration and spreading (56, 57), did not promote the plasma membrane recruitment of Radil (supplemental Fig. 1). To quantitatively support our immunofluorescence data, we performed biochemical fractionation experiments. Although a modest amount of Venus-Radil was found in the membrane pool under resting conditions, expression of Rap1aQ63E and Gβγ markedly promoted the association of Radil with the membrane fractions (Fig. 3*B*, compare *lanes 2* and *3* with *lane 1*). We, thus, conclude that after Gβγ and Rap1a activation, the Rap effector Radil is translocated to the plasma membrane at sites of cell-matrix contacts likely through the formation of the Gβγ·Rap1·Radil protein complex.

The Gβγ·Rap1·Radil Complex Regulates Cell Spreading and Cell-Matrix Adhesiveness—Research in the last 10 years has established Rap1a as an important factor in the regulation of cell-matrix and cell-cell adhesion (58–60). Rap1a activation has been implicated in inside-out signaling leading to the activation of integrins and increases in cell-matrix adhesion (42, 58–61). Radil was recently described as a Rap effector with a role in the control of cell-matrix adhesion (40). Consistent with these notions, we noted that overexpression of WT or constitutively active Rap1a or Radil led to increased cell spreading (Fig. 4, *A* and *B*), a phenotype commonly associated with increased cell-matrix adhesiveness (55). Interestingly, the overexpression of Gβγ also led to an increased spreading of these cells (Fig. 4, *A* and *B*). To quantitatively monitor the effects of Rap1a, Radil, or Gβγ overexpression on the spreading of HT1080 cells in real time, we employed the xCELLigence impedance system (62). This system provides a cell index that increases as a function of cell attachment, spreading, and cell growth. As Fig. 4*C* shows, the overexpression of Rap1WT, Gβγ, Radil, and Rap1aQ63E led to progressively higher cell indices compared with control-transfected cells over the first 2 h. We conclude that the induced formation of the Gβγ·Rap1·Radil complex increases the spreading of HT1080 cells.

These results led us to test the hypothesis that the Gβγ·Rap1a·Radil protein complex may represent a cellular machinery regulating cell adhesion downstream of GPCR activity. To test this we optimized a cell-matrix adhesion assay to measure the adhesion of HT1080 cells to the extracellular matrix protein fibronectin. In this assay, overexpression of Rap1aQ63E predictably led (as it promotes inside-out integrin signaling) to a strong increase in the adhesive properties of these cells (Fig. 5*A*, quantified in Fig. 5*B*). Inhibiting Rap1a activation by expressing Rap1GAP on the other hand did not lead to any increase in cell adhesion.

After having determined the dynamic range of this assay, we tested whether the overexpression of the other members of the Gβγ·Rap1a·Radil complex was sufficient to promote adhesion of these cells. Both Radil or Gβγ overexpression led to a strong potentiation of cell-matrix adhesion (Fig. 5, *A* and *B*) to levels similar to that observed with Rap1aQ63E expression (Fig. 5, *A* and *B*). Consistent with the interaction data between Gβγ,

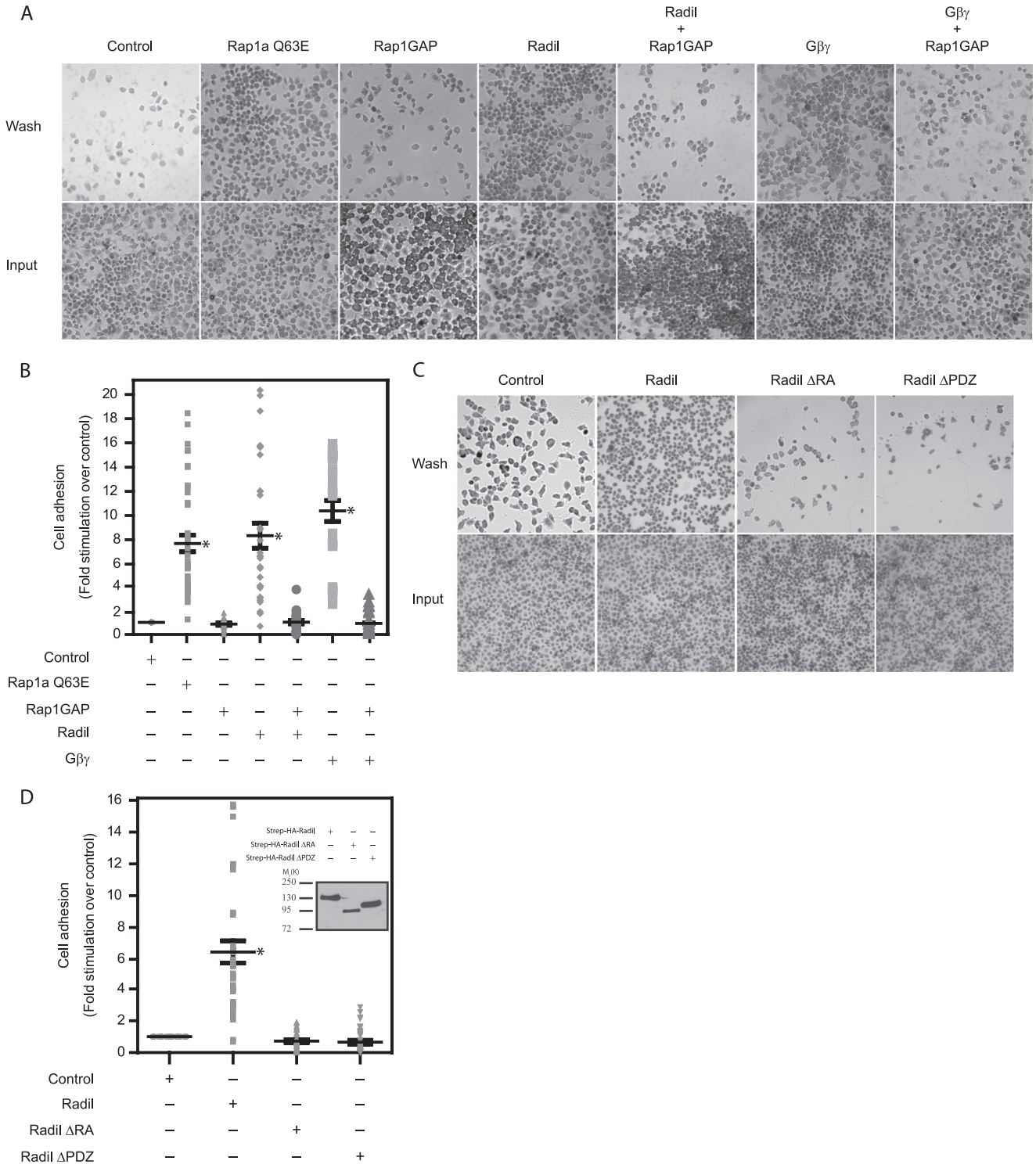

FIGURE 5. **Radil and Gβγ promote adhesion of HT1080 cells on fibronectin matrix in a Rap1a dependent manner.** *A*, shown are representative pictures of HT1080 cell adhesion assays in response to overexpression of different proteins as indicated. FLAG-GFP cDNA was transfected as control. *Top panels* show the remaining adherent cells after washes. The *bottom panels* demonstrate the total cells input for each conditions. *B*, shown is a quantified representation of the adhesion assay as -fold stimulation compared with control. *C*, shown are representative pictures comparing the ability of ΔRA and ΔPDZ Radil mutants to promote HT1080 cells adhesion. *D*, shown is a quantified representation of *C*. The *inset* shows expression of the different Radil proteins in one representative experiment. Each experiment was done in triplicate, and several pictures from random fields were taken from each well of 96-well plate. Cells were counted (using an automated cell counting macro created in ImageJ software) from each field and expressed as -fold of control from each experiment. The results from three independent experiments were pooled for the quantification. Each dot on the graph represents cell counts from a single field. *Error bars*, ±S.E. Statistics are one-way ANOVA followed by Tukey's multiple comparison test; $p < 0.05$. *Asterisks* indicate statistical significance compared with control.

Radil, and Rap1a (Fig. 2*B*), the increase in adhesion promoted by Radil or Gβγ expression depended on Rap1a activity. Indeed, coexpression of Rap1GAP strongly inhibited both Gβγ- or Radil-promoted cell-matrix adhesion (Fig. 5, *A* and *B*). We conclude that the Gβγ·Rap1a·Radil protein complex is sufficient to promote cell-matrix adhesiveness.

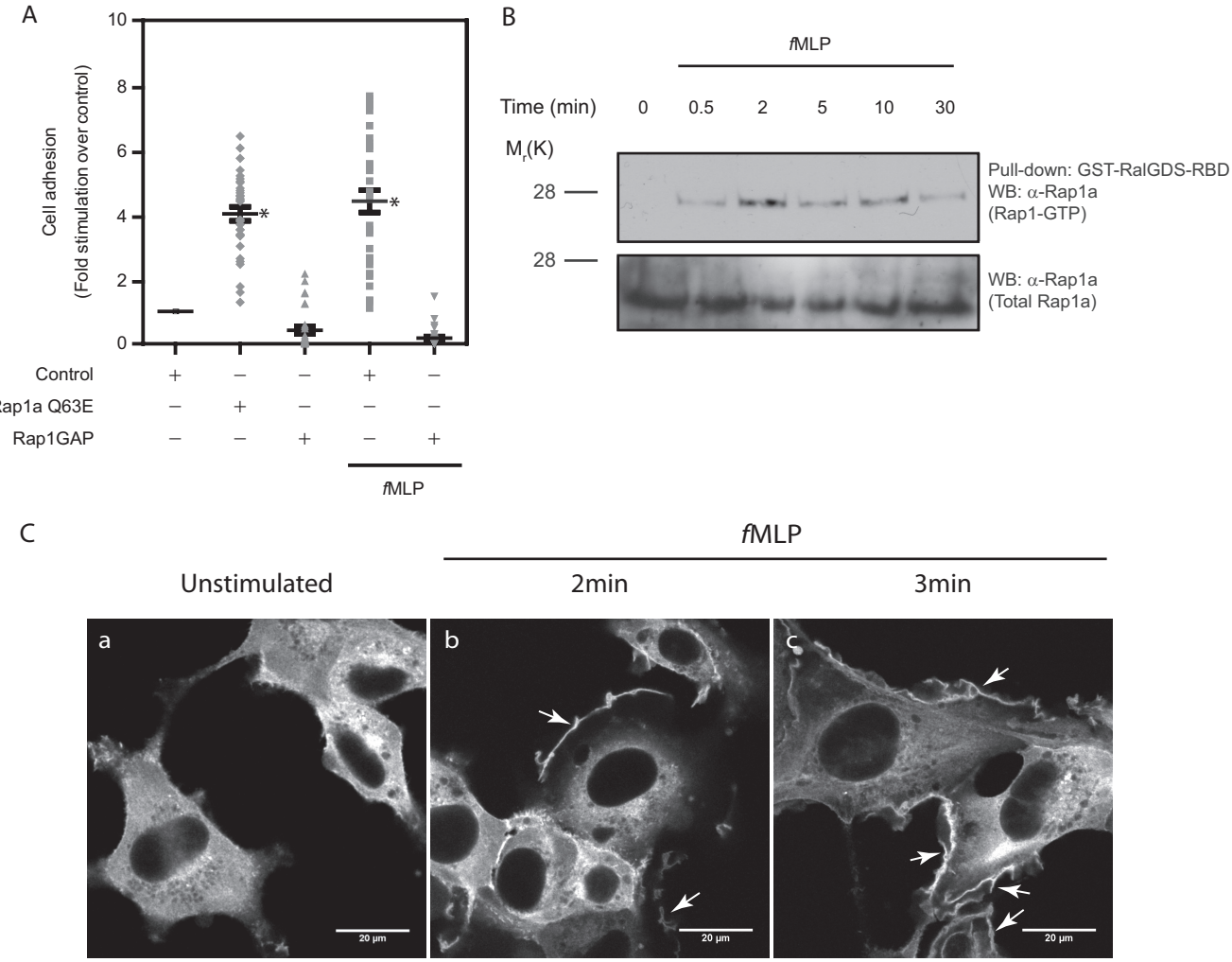

FIGURE 6. **fMLP promotes Rap1-dependent HT1080 cell adhesion, Rap1 activation, and Radil translocation to the plasma membrane.** *A*, HT1080 cell adhesion on a fibronectin matrix is shown with or without *f*MLP (100 nM) stimulation in the presence or absence of Rap1GAP. Rap1aQ63E (used as a positive control) shows the increase in cell adhesion ($n = 3$). *B*, shown is the time course of Rap1 activation by fMLP (100 nM) in HT1080 cells. The *top panel* shows GTP-bound Rap1a, purified using GST-RalGDS-RBD pulldown assays. The *bottom panel* shows total Rap1 in a fraction of whole cell lysates from each sample. Western blotting (*WB*) was done using α-Rap1a antibodies. *C*, HT1080 cells stably expressing Venus-Radil were serum-starved for 24 h and stimulated or not with fMLP (1 μM) for 0 min (*a*), 2 min (*b*), 3 min (*c*) at 37 °C. *Arrows* highlight regions of Venus-Radil enrichment at the plasma membrane. Images were captured by a blinded observer using 100× oil-immersion lens. Images shown are representative of two independent experiments. *Bars*, 20 μm.

As stated previously, Radil is composed of RA, DIL, and PDZ domains. We next studied the individual requirement of the RA and PDZ domains of Radil for their ability to promote cell-matrix adhesion. Whereas overexpression of full-length Radil led to a robust increase in adhesion (Fig. 5, *C* and *D*), equivalent expression (Fig. 5*D*, *inset*) of ΔRA or ΔPDZ mutant Radil proteins had no effect. Because the RA domain is known to interact with GTP-bound Rap1a, these results further support the requirement for the Rap1a-Radil interaction for this process and indicate that the PDZ domain is also required possibly through the interaction of an as yet unidentified PDZ ligand-containing effector protein.

GPCR Activation Leads to Rap1 Activation, Radil Translocation to the Plasma Membrane, and Increased Cell-Matrix Adhesion—Having established that the formation of the Gβγ·Rap1a·Radil protein complex was sufficient to promote cell-matrix adhesion, we next wanted to assess its requirement in the context of a GPCR known to modulate cell adhesion. A previous report described that HT1080 cells endogenously express functional formyl peptide receptors (FPRs) and that their activation with the formylated peptide fMLP strongly potentiates cell matrix adhesion (63). We first repeated this experiment and showed that fMLP treatment of these cells also caused an ~5-fold increase in adhesion using our experimental conditions (Fig. 6*A*). We next asked whether fMLP-promoted cell adhesion requires active Rap1a. To do this we overexpressed Rap1GAP and asked whether fMLP could still potentiate adhesion. As shown in Fig. 6*A*, expression of Rap1GAP strongly antagonized the ability of fMLP to induce cell adhesion. We conclude that FPRs utilize a Rap1a-dependent pathway to regulate cell adhesion to the fibronectin matrix. Supporting this, fMLP treatment of these cells led to a rapid and robust activation of Rap1a (Fig. 6*B*). This activation was sustained, peaked at 2 min, and slowly waned over time. Learning from the localization experiments (Fig. 3) that activated Rap1 and Gβγ translocates Radil to the plasma membrane, we tested the prediction that fMLP treatment of the cells would also lead to a translocation of Radil to the plasma membrane. As shown

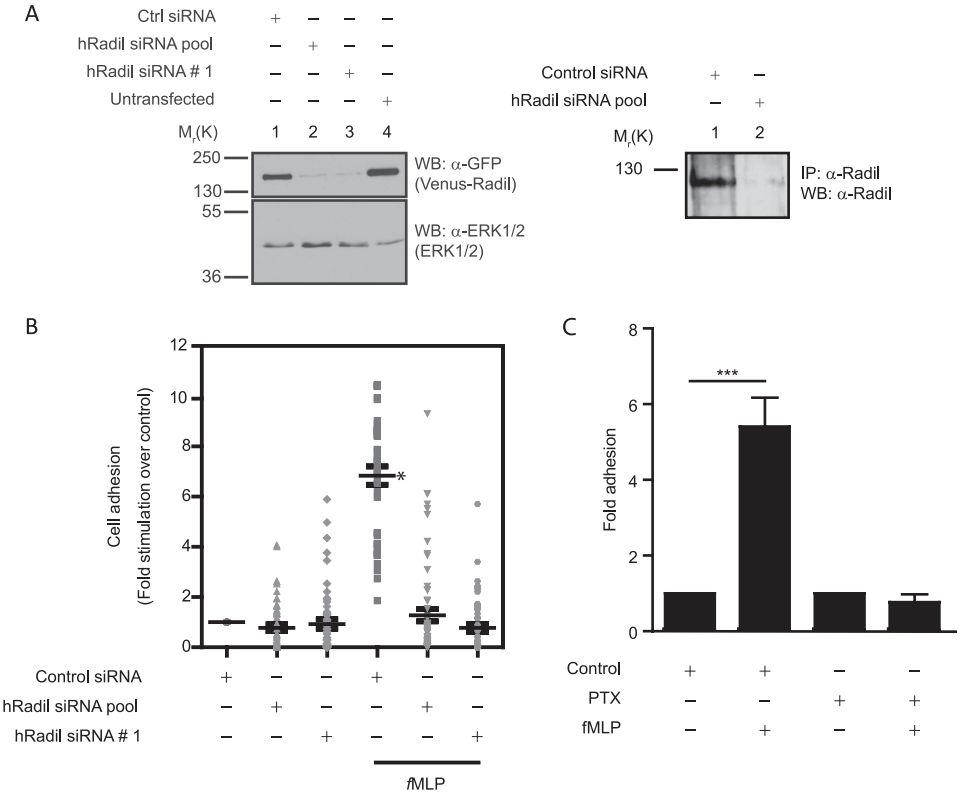

FIGURE 7. **Radil is required for the fMLP-promoted HT1080 cell adhesion on fibronectin matrix.** *A*, shown is efficiency of Radil knockdown. HT1080 cells stably expressing Venus-Radil were treated with control, a pool of four Radil siRNAs (hRadil siRNA pool), or a single Radil siRNA (hRadil siRNA #1) (*left panel*), and Radil expression was monitored by Western blot (*IP*) using GFP antibodies. Immunoblotting with total Erk1/2 antibodies was performed as loading controls. Endogenous hRadil knockdown efficiency in HT1080 cells using the hRadil siRNA pool is shown in the *right panel*. Cells transfected with control or hRadil siRNA pool were lysed, and equivalent amounts of lysates were immunoprecipitated (*IP*) using α-Radil rabbit polyclonal antibodies followed by detection in Western blot using the same antibody. *B*, shown is fMLP-promoted cell adhesion in HT1080 cells treated with control or hRadil siRNAs ($n = 4$). Each dot on the graph represents counts from a single field. The *asterisk* indicates statistical significance compared with control treatment. *C*, treatment of HT1080 cells with PTX (100 ng/ml) inhibits fMLP-mediated cell adhesion. Each experiment was done in triplicate, and several pictures from random fields were taken from each well of a 96-well plate. Cells were counted from each field and expressed as -fold of control from each experiment. Data from all experiments were pooled. *Error bars*, ±S.E. Statistical significance was assessed using one-way ANOVA followed by post-hoc analysis using Tukey's multiple comparison test; $p < 0.05$.

in Fig. 6*C*, Venus-Radil was enriched at the plasma membrane within 2–3 min after FPR activation, a kinetic that mirrored Rap1a activation. We conclude that FRP activation by fMLP leads to Rap1a activation and to the recruitment of Radil to the plasma membrane.

The Gβγ·Rap1a·Radil Signaling Axis Regulates Adhesion Downstream of GPCR Activation—Our next goal was to determine whether Radil was required downstream of FPR activation for the control of cell adhesion using a RNAi loss of function approach. We first validated the efficiency of a pool of four individual siRNA sequences targeting Radil to inhibit the expression of Venus-Radil (Fig. 7*A*, *left blot* compare *lanes 2* and *1*) and more importantly to target the levels of endogenous Radil proteins in HT1080 cells (Fig. 7*A*, *right blot*). Using these reagents we then assessed the ability of fMLP to promote cell-matrix adhesion when Radil levels are reduced. Whereas control and Radil siRNA-treated cells exhibited background levels of adhesion on their own, Radil siRNAs strongly inhibited the ability of fMLP to promote adhesion when compared with control siRNA-treated cells (Fig. 7*B*). Importantly, we also screened several individual Radil siRNAs and found one (Radil siRNA#1) that effectively targeted Radil expression (Fig. 7*A*, compare *lanes 3* and *1*). Similar results were obtained using this single siRNA in the functional adhesion assay (Fig. 7*B*). To evaluate the implication of $G\alpha_i$-containing heterotrimeric G proteins for the fMLP-promoted increase in adhesion, we pretreated the cells with 100 ng/ml of PTX for 16 h, a concentration known to inactivate $G\alpha_i$. Although fMLP induced the expected 5-fold increase in control-treated cells, PTX completely inhibited fMLP-mediated cell adhesion (Fig. 7*C*). We conclude from these results that a $G\alpha_i$-containing heterotrimeric G protein and Radil are required downstream of FPRs for the control of cell-matrix adhesion.

The Gβγ·Rap1a·Radil Complex Regulates Inside-out Signaling Leading to Integrin Activation—We were then interested in addressing the mechanism by which GPCR activation and the Gβγ·Rap1a·Radil complex modulate cell adhesion. Cell-matrix adhesiveness is a dynamic process regulated through the interaction of integrin receptors with extracellular matrix components. Both integrin availability and affinity for their ligands can be regulated. The latter has been shown to be controlled in part by signaling through the small GTPase Rap1a in a process known as inside-out signaling (64–66). HT1080 cells are known to express several integrins including the $\alpha5\beta1$ subtypes that form the receptor for fibronectin. Because GPCRs have previously been shown to regulate integrin affinity (30, 67, 68), we investigated whether the Gβγ·Radil·Rap1a protein complex regulates cell-matrix adhesion through inside-out signaling and integrin activation. To perform this experiment we took advantage of a conformationally sensitive monoclonal antibody (9EG7) that selectively recognizes β1-integrin when activated (69, 70) and initially asked whether Rap1aQ63E, Radil, or Gβγ overexpression or fMLP treatment led to integrin activation. When expressed in HT1080 cells, these proteins increased cell spreading (Fig. 4) and adhesion (Fig. 5). After expression of these proteins or treatment of the cells with fMLP, a substantial increase in β1-integrin activation was measured (Fig. 8, *A* and *B*) to levels approaching 50–60% that obtained after treatment of the cells with the divalent cation Mn^{2+} used as a positive control to maximally activate integrins. Importantly and consistent with the requirement of activated Rap1a for the

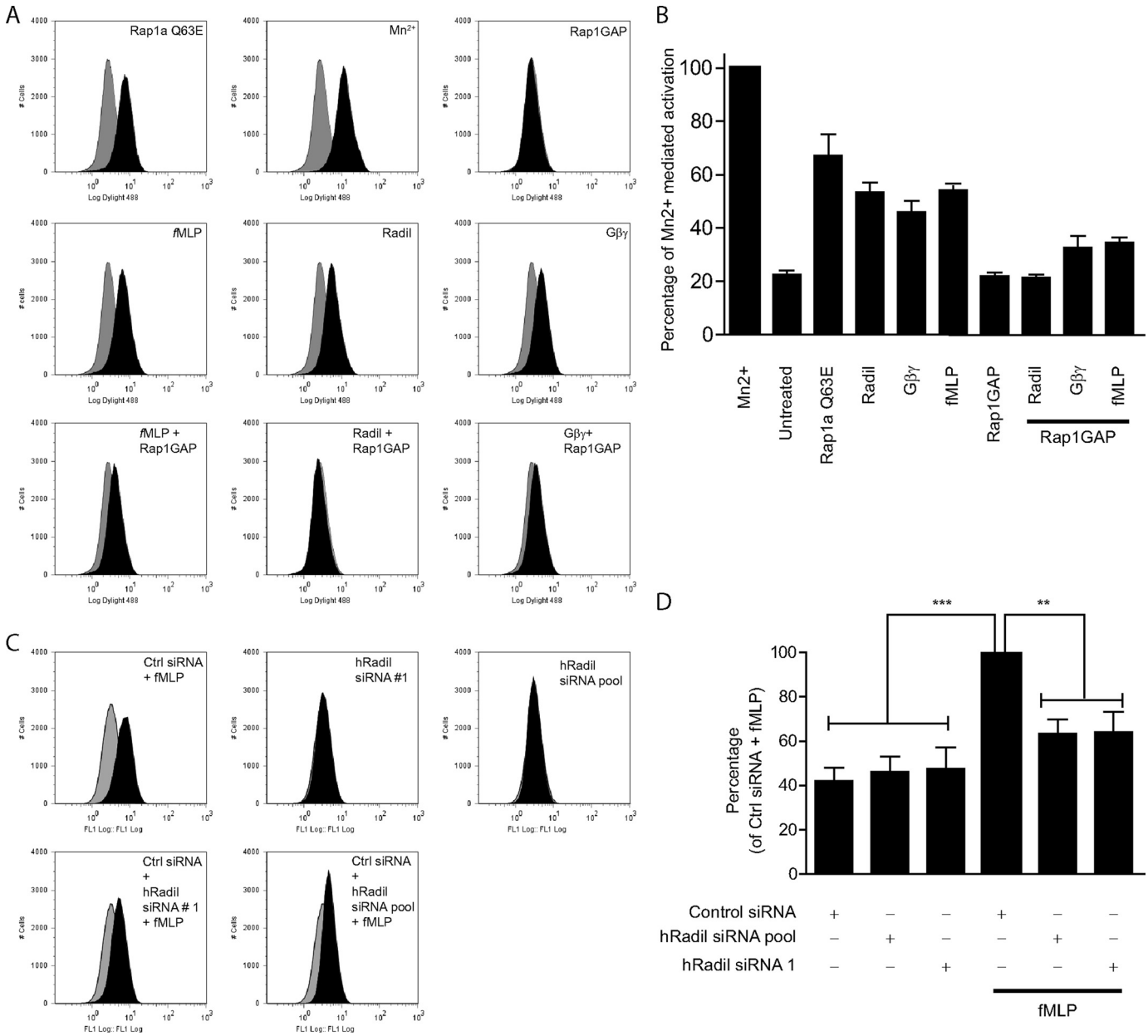

FIGURE 8. **β1 integrin activation.** *A*, representative flow cytometry analysis shows β1 integrin activation upon the indicated treatments. The *gray area* represents control staining with 9EG7 monoclonal antibody antibodies that specifically recognize activated β1-integrins. The *black area* corresponds to the treated population. Rap1aQ63E, Mn^{2+v} and Rap1GAP are used as controls. *B*, shown is the average of three independent experiments performed as in *A* showing β1 integrin activation upon the different treatments. *Error bars*, ± S.E. *C*, flow cytometry analysis shows β1 integrin activation in the presence or absence of *f*MLP in HT1080 cells treated with control (*Ctrl*) or hRadil siRNAs. *D*, shown is the average of three independent experiments performed as in *C*. *Error bars*, ±S.E. Statistics are one-way ANOVA followed by post-hoc analysis using Tukey's multiple comparison test; $p < 0.05$.

Gβγ·Rap1a·Radil complex assembly and function, the overexpression of Rap1GAP inhibited integrin activation in each case (Fig. 8, *A* and *B*).

To address the requirement for Radil in fMLP-induced integrin activation, we treated HT1080 cells with control or two independent Radil siRNAs and compared integrin activation patterns upon fMLP stimulation. Although fMLP promoted integrin activation by ~3-fold in control siRNA-treated cells, depletion of Radil severely impaired the ability of fMLP to activate integrins (Fig. 8, *C* and *D*) but did not affect the Mn^{2+} response (data not shown). These findings support the view that the Gβγ·Radil·Rap1a complex controls cell adhesiveness downstream of GPCR activation by regulating inside-out signaling leading to integrin activation.

DISCUSSION

Several GPCRs have been implicated in the control of cell motility and adhesion. However, the intracellular signaling pathways underlying these functions remain poorly defined. We present here the functional characterization of a novel protein complex functioning downstream of GPCR signaling to regulate cell-matrix adhesion. We have identified Radil, a Rap1 effector, as a multidomain protein linking GPCRs, Gβγ, and Rap1-GTP to integrin activation. First, Gβγ or Radil overex-

pression is sufficient to activate mesenchymal cell spreading and adhesion to fibronectin and to promote the active conformation of integrins. Second, Gβγ and active Rap1a promote the localization of Radil to sites of cell-matrix adhesion within the plasma membrane. Third, the stimulation of cell adhesion by fMLP receptors was abrogated in Radil knockdown cells and when Rap1a function was inhibited with the overexpression of Rap1GAP. Our results, thus, unveil a new signaling axis downstream of Rap1 activation by GPCRs and implicate a function for the Gβγ·Rap1a·Radil protein complex in the inside-out signaling cascade leading to integrin activation.

Other Rap1 effectors have previously been identified and shown to be important in regulating cell adhesion. RAPL, which is enriched in lymphoid tissues, has been shown to be important for the polarized relocalization of LFA1, the major leukocyte integrin (33), to the leading edge. Another effector important for T cell functions is RIAM, which regulates adhesion by the modulation of actin dynamics through its interaction with Profilin and Ena/Vasp proteins (28). Similar to Radil, overexpression of RAPL or RIAM also leads to enhanced adhesion and integrin activation (29, 33). Additional studies will be needed to understand how Rap1 selectively activates different effectors in different contexts. One possibility is that the expression of the different Rap1 effectors is restricted to specific cell types. Supporting this, RAPL and RIAM are expressed highly in lymphoid cells but are either absent or expressed at low levels in other cell types (28, 33). Although Radil is expressed in all epithelial and fibroblast cell lines that we examined (data not shown) and is broadly expressed in zebrafish embryos (40), we do not know its level of expression in lymphocytes and whether it is functionally redundant with RAPL or RIAM in this setting. Alternatively, the recruitment of Rap1 and one of its effectors within a protein complex could account for the specificity of action. GPCR-activated Gβγ subunits in this design could serve to insulate the activation of Radil from the other Rap1 effectors after Rap1 activation. Supporting this possibility, we found that Gβγ interacts with Radil but not with its close homologue AF-6 (Fig. 1*C*).

Because Rap1 regulates cell-cell and cell-matrix adhesion in different contexts, its role in tumorigenesis and cancer progression has been closely scrutinized (71–74). Recent findings suggest a role for aberrant Rap1 activity in prostate cancer progression, as activation of Rap1 increased prostate cancer cell migration and invasion, and its inhibition had the opposite effect (75). Interestingly, in the same study integrins were shown to be involved in the mechanism of Rap1-mediated migration and invasion of prostate cancer cells. Further supporting a role for Rap1 activation for cancer dissemination, Rap1GAP expression has been found to be down-regulated in several cancers (76–78). Roles for Rap1 effectors in the context of cancers have not been explored. As mentioned earlier, Radil was originally identified as a factor induced by a chromosomal translocation in a sarcoma (40). Interestingly, a recent analysis of prostate cancer biopsies demonstrated that Radil expression is up-regulated during prostate cancer progression (79). Together this suggests that Rap1 signaling through Radil may be important for cancer initiation/progression. Given Radil assembly in the Gβγ·Rap1·Radil complex, the role of Radil may, thus, be particularly important in the context of GPCR signaling during metastasis. Indeed, chemokine receptors for example are known to direct tumor cells metastasis and tropism to different secondary sites. Further studies examining the role of this protein complex during the progression of different cancers are, thus, needed.

This study unveils a previously unappreciated role for Gβγ in regulating cell adhesion through its recruitment in the Gβγ·Rap1·Radil complex. Given that the formation of this protein complex requires the activation of Rap1, one function for this complex, which we characterized in the present study, occurs downstream of Rap1 activation by GPCRs. One important question that remains unclear and that was beyond the focus of our study is how GPCRs lead to Rap1 activation. Further studies are, thus, needed to precisely map the sequence of events leading to Rap1 activation by GPCRs and to evaluate whether context-dependent signaling pathways may contribute to Rap activation and engagement of the Gβγ·Rap1·Radil complex to regulate cell adhesion.

In conclusion, this study identifies the Gβγ·Rap1·Radil complex as an important component of GPCR signaling regulating cell-matrix adhesion. Although we found that Radil leads to integrins activation, how exactly Radil regulates this process and whether it has other functions is not known. Perhaps the identification of which PDZ ligand containing binding partners interacts with Radil will help to further understand how this protein complex works. Because Rap1 is also known to function in cell-cell adhesion and cell invasion, which are also known to be regulated by GPCR signaling, more work is also needed to examine the role of the Gβγ·Rap1·Radil complex in these processes.

Acknowledgments—We are grateful to Drs. Carole Parent, Terry Hebert, Ali Salahpour, and Stéphanie Pontier as well as members of the Angers laboratory for discussions and critical reading of the manuscript.

REFERENCES

1. Doitsidou, M., Reichman-Fried, M., Stebler, J., Köprunner, M., Dörries, J., Meyer, D., Esguerra, C. V., Leung, T., and Raz, E. (2002) *Cell* **111,** 647–659
2. Scott, I. C., Masri, B., D'Amico, L. A., Jin, S. W., Jungblut, B., Wehman, A. M., Baier, H., Audigier, Y., and Stainier, D. Y. (2007) *Dev. Cell* **12,** 403–413
3. Carmona, G., Chavakis, E., Koehl, U., Zeiher, A. M., and Dimmeler, S. (2008) *Blood* **111,** 2640–2646
4. Servant, G., Weiner, O. D., Herzmark, P., Balla, T., Sedat, J. W., and Bourne, H. R. (2000) *Science* **287,** 1037–1040
5. Höpken, U. E., Lu, B., Gerard, N. P., and Gerard, C. (1996) *Nature* **383,** 86–89
6. Snyderman, R., and Goetzl, E. J. (1981) *Science* **213,** 830–837
7. Sambrano, G. R., Weiss, E. J., Zheng, Y. W., Huang, W., and Coughlin, S. R. (2001) *Nature* **413,** 74–78
8. Kahn, M. L., Zheng, Y. W., Huang, W., Bigornia, V., Zeng, D., Moff, S., Farese, R. V., Jr., Tam, C., and Coughlin, S. R. (1998) *Nature* **394,** 690–694
9. Komarova, Y. A., Mehta, D., and Malik, A. B. (2007) *Sci. STKE 2007*, re8
10. Baggiolini, M. (1998) *Nature* **392,** 565–568
11. Askari, J. A., Buckley, P. A., Mould, A. P., and Humphries, M. J. (2009) *J. Cell Sci.* **122,** 165–170
12. Tiveron, M. C., and Cremer, H. (2008) *Curr. Opin. Neurobiol.* **18,** 237–244
13. Offermanns, S. (2006) *Circ. Res.* **99,** 1293–1304
14. Druey, K. M. (2009) *Immunol. Res.* **43,** 62–76
15. Fraser, C. C. (2008) *Int. Rev. Immunol.* **27,** 320–350

16. Rozengurt, E. (2007) *J. Cell. Physiol.* **213,** 589–602
17. Lattin, J., Zidar, D. A., Schroder, K., Kellie, S., Hume, D. A., and Sweet, M. J. (2007) *J. Leukocyte Biol.* **82,** 16–32
18. Müller, A., Homey, B., Soto, H., Ge, N., Catron, D., Buchanan, M. E., McClanahan, T., Murphy, E., Yuan, W., Wagner, S. N., Barrera, J. L., Mohar, A., Verástegui, E., and Zlotnik, A. (2001) *Nature* **410,** 50–56
19. Dankort, D., Maslikowski, B., Warner, N., Kanno, N., Kim, H., Wang, Z., Moran, M. F., Oshima, R. G., Cardiff, R. D., and Muller, W. J. (2001) *Mol. Cell. Biol.* **21,** 1540–1551
20. Mills, G. B., and Moolenaar, W. H. (2003) *Nat. Rev. Cancer* **3,** 582–591
21. Guillermet-Guibert, J., Bjorklof, K., Salpekar, A., Gonella, C., Ramadani, F., Bilancio, A., Meek, S., Smith, A. J., Okkenhaug, K., and Vanhaesebroeck, B. (2008) *Proc. Natl. Acad. Sci. U.S.A.* **105,** 8292–8297
22. Stoyanov, B., Volinia, S., Hanck, T., Rubio, I., Loubtchenkov, M., Malek, D., Stoyanova, S., Vanhaesebroeck, B., Dhand, R., and Nürnberg, B. (1995) *Science* **269,** 690–693
23. N'Diaye, E. N., and Brown, E. J. (2003) *J. Cell Biol.* **163,** 1157–1165
24. Faivre, S., Régnauld, K., Bruyneel, E., Nguyen, Q. D., Mareel, M., Emami, S., and Gespach, C. (2001) *Mol. Pharmacol.* **60,** 363–372
25. Ginsberg, M. H., Partridge, A., and Shattil, S. J. (2005) *Curr. Opin. Cell Biol.* **17,** 509–516
26. Takagi, J., Petre, B. M., Walz, T., and Springer, T. A. (2002) *Cell* **110,** 599–611
27. Lafuente, E. M., Iwamoto, Y., Carman, C. V., van Puijenbroek, A. A., Constantine, E., Li, L., and Boussiotis, V. A. (2007) *Leuk. Lymphoma* **48,** 987–1002
28. Lafuente, E. M., van Puijenbroek, A. A., Krause, M., Carman, C. V., Freeman, G. J., Berezovskaya, A., Constantine, E., Springer, T. A., Gertler, F. B., and Boussiotis, V. A. (2004) *Dev. Cell* **7,** 585–595
29. Watanabe, N., Bodin, L., Pandey, M., Krause, M., Coughlin, S., Boussiotis, V. A., Ginsberg, M. H., and Shattil, S. J. (2008) *J. Cell Biol.* **181,** 1211–1222
30. Laudanna, C., Kim, J. Y., Constantin, G., and Butcher, E. (2002) *Immunol. Rev.* **186,** 37–46
31. Ley, K., Laudanna, C., Cybulsky, M. I., and Nourshargh, S. (2007) *Nat. Rev. Immunol.* **7,** 678–689
32. Zarbock, A., Polanowska-Grabowska, R. K., and Ley, K. (2007) *Blood Rev.* **21,** 99–111
33. Katagiri, K., Maeda, A., Shimonaka, M., and Kinashi, T. (2003) *Nat. Immunol.* **4,** 741–748
34. Angers, S., Thorpe, C. J., Biechele, T. L., Goldenberg, S. J., Zheng, N., MacCoss, M. J., and Moon, R. T. (2006) *Nat. Cell Biol.* **8,** 348–357
35. Angers, S., Li, T., Yi, X., MacCoss, M. J., Moon, R. T., and Zheng, N. (2006) *Nature* **443,** 590–593
36. Magga, J. M., Jarvis, S. E., Arnot, M. I., Zamponi, G. W., and Braun, J. E. (2000) *Neuron* **28,** 195–204
37. Dupré, D. J., Robitaille, M., Richer, M., Ethier, N., Mamarbachi, A. M., and Hébert, T. E. (2007) *J. Biol. Chem.* **282,** 13703–13715
38. Humrich, J., Bermel, C., Bünemann, M., Härmark, L., Frost, R., Quitterer, U., and Lohse, M. J. (2005) *J. Biol. Chem.* **280,** 20042–20050
39. Willardson, B. M., and Howlett, A. C. (2007) *Cell. Signal.* **19,** 2417–2427
40. Smolen, G. A., Schott, B. J., Stewart, R. A., Diederichs, S., Muir, B., Provencher, H. L., Look, A. T., Sgroi, D. C., Peterson, R. T., and Haber, D. A. (2007) *Genes Dev.* **21,** 2131–2136
41. Zhang, Z., Rehmann, H., Price, L. S., Riedl, J., and Bos, J. L. (2005) *J. Biol. Chem.* **280,** 33200–33205
42. Kooistra, M. R., Dubé, N., and Bos, J. L. (2007) *J. Cell Sci.* **120,** 17–22
43. Su, L., Hattori, M., Moriyama, M., Murata, N., Harazaki, M., Kaibuchi, K., and Minato, N. (2003) *J. Biol. Chem.* **278,** 15232–15238
44. Rubinfeld, B., Munemitsu, S., Clark, R., Conroy, L., Watt, K., Crosier, W. J., McCormick, F., and Polakis, P. (1991) *Cell* **65,** 1033–1042
45. Jeon, T. J., Lee, D. J., Lee, S., Weeks, G., and Firtel, R. A. (2007) *J. Cell Biol.* **179,** 833–843
46. Bos, J. L., Franke, B., M'Rabet, L., Reedquist, K., and Zwartkruis, F. (1997) *FEBS Lett.* **410,** 59–62
47. Feller, S. M., Posern, G., Voss, J., Kardinal, C., Sakkab, D., Zheng, J., and Knudsen, B. S. (1998) *J. Cell. Physiol.* **177,** 535–552
48. Carey, K. D., Dillon, T. J., Schmitt, J. M., Baird, A. M., Holdorf, A. D., Straus, D. B., Shaw, A. S., and Stork, P. J. (2000) *Mol. Cell. Biol.* **20,** 8409–8419
49. Durand, C. A., Westendorf, J., Tse, K. W., and Gold, M. R. (2006) *Eur. J. Immunol.* **36,** 2235–2249
50. McLeod, S. J., Li, A. H., Lee, R. L., Burgess, A. E., and Gold, M. R. (2002) *J. Immunol.* **169,** 1365–1371
51. Citro, S., Malik, S., Oestreich, E. A., Radeff-Huang, J., Kelley, G. G., Smrcka, A. V., and Brown, J. H. (2007) *Proc. Natl. Acad. Sci. U.S.A.* **104,** 15543–15548
52. Bivona, T. G., Wiener, H. H., Ahearn, I. M., Silletti, J., Chiu, V. K., and Philips, M. R. (2004) *J. Cell Biol.* **164,** 461–470
53. Li, Y., Asuri, S., Rebhun, J. F., Castro, A. F., Paranavitana, N. C., and Quilliam, L. A. (2006) *J. Biol. Chem.* **281,** 2506–2514
54. Boettner, B., Govek, E. E., Cross, J., and Van Aelst, L. (2000) *Proc. Natl. Acad. Sci. U.S.A.* **97,** 9064–9069
55. Arthur, W. T., Quilliam, L. A., and Cooper, J. A. (2004) *J. Cell Biol.* **167,** 111–122
56. Niggli, V., Schlicht, D., and Affentranger, S. (2009) *Biochem. Biophys. Res. Commun.* **386,** 688–692
57. Fukata, M., Nakagawa, M., and Kaibuchi, K. (2003) *Curr. Opin. Cell Biol.* **15,** 590–597
58. Bos, J. L. (2005) *Curr. Opin. Cell Biol.* **17,** 123–128
59. Bos, J. L., de Bruyn, K., Enserink, J., Kuiperij, B., Rangarajan, S., Rehmann, H., Riedl, J., de Rooij, J., van Mansfeld, F., and Zwartkruis, F. (2003) *Biochem. Soc. Trans.* **31,** 83–86
60. Bos, J. L., de Rooij, J., and Reedquist, K. A. (2001) *Nat. Rev. Mol. Cell Biol.* **2,** 369–377
61. Reedquist, K. A., Ross, E., Koop, E. A., Wolthuis, R. M., Zwartkruis, F. J., van Kooyk, Y., Salmon, M., Buckley, C. D., and Bos, J. L. (2000) *J. Cell Biol.* **148,** 1151–1158
62. Atienza, J. M., Zhu, J., Wang, X., Xu, X., and Abassi, Y. (2005) *J. Biomol. Screen* **10,** 795–805
63. VanCompernolle, S. E., Clark, K. L., Rummel, K. A., and Todd, S. C. (2003) *J. Immunol.* **171,** 2050–2056
64. Mor, A., Dustin, M. L., and Philips, M. R. (2007) *Immunol. Rev.* **218,** 114–125
65. Banno, A., and Ginsberg, M. H. (2008) *Biochem. Soc. Trans.* **36,** 229–234
66. Kinbara, K., Goldfinger, L. E., Hansen, M., Chou, F. L., and Ginsberg, M. H. (2003) *Nat. Rev. Mol. Cell Biol.* **4,** 767–776
67. Etzioni, A., and Alon, R. (2004) *Curr. Opin. Allergy Clin. Immunol.* **4,** 485–490
68. Alon, R., and Ley, K. (2008) *Curr. Opin. Cell Biol.* **20,** 525–532
69. Bazzoni, G., Shih, D. T., Buck, C. A., and Hemler, M. E. (1995) *J. Biol. Chem.* **270,** 25570–25577
70. Wei, Y., Czekay, R. P., Robillard, L., Kugler, M. C., Zhang, F., Kim, K. K., Xiong, J. P., Humphries, M. J., and Chapman, H. A. (2005) *J. Cell Biol.* **168,** 501–511
71. Hattori, M., and Minato, N. (2003) *J. Biochem.* **134,** 479–484
72. Till, K. J., Harris, R. J., Linford, A., Spiller, D. G., Zuzel, M., and Cawley, J. C. (2008) *Cancer Res.* **68,** 8429–8436
73. Hao, J. J., Wang, G., Pisitkun, T., Patino-Lopez, G., Nagashima, K., Knepper, M. A., Shen, R. F., and Shaw, S. (2008) *J. Proteome Res.* **7,** 2911–2927
74. Itoh, M., Nelson, C. M., Myers, C. A., and Bissell, M. J. (2007) *Cancer Res.* **67,** 4759–4766
75. Bailey, C. L., Kelly, P., and Casey, P. J. (2009) *Cancer Res.* **69,** 4962–4968
76. Nellore, A., Paziana, K., Ma, C., Tsygankova, O. M., Wang, Y., Puttaswamy, K., Iqbal, A. U., Franks, S. R., Lv, Y., Troxel, A. B., Feldman, M. D., Meinkoth, J. L., and Brose, M. S. (2009) *J. Clin. Endocrinol. Metab.* **94,** 1026–1032
77. Zhang, L., Chenwei, L., Mahmood, R., van Golen, K., Greenson, J., Li, G., D'Silva, N. J., Li, X., Burant, C. F., Logsdon, C. D., and Simeone, D. M. (2006) *Cancer Res.* **66,** 898–906
78. Tsygankova, O. M., Prendergast, G. V., Puttaswamy, K., Wang, Y., Feldman, M. D., Wang, H., Brose, M. S., and Meinkoth, J. L. (2007) *Mol. Cell. Biol.* **27,** 6647–6658
79. Savli, H., Szendröi, A., Romics, I., and Nagy, B. (2008) *Exp. Mol. Med.* **40,** 176–185